Available online at www.sciencedirect.com

ScienceDirect

Procedia Manufacturing 50 (2020) 584–588

Procedia MANUFACTURING

www.elsevier.com/locate/procedia

18th International Conference Metal Forming 2020

A study on ratio and linearity of strain path in in-plane biaxial tensile test for formability evaluation

Ruiqiang Zhang[a,]*, Zhutao Shao[a], Zhusheng Shi[a], Jianguo Lin[a]

[a]*Department of Mechanical Engineering, Imperial College London, London and SW7 2AZ, UK*

* Corresponding author. *E-mail address:* r.zhang17@imperial.ac.uk

Abstract

In-plane biaxial tensile test is an alternative to determine the forming limit diagram (FLD) for evaluating the formability of metal sheets, in which cruciform specimens are deformed under the plane stress condition. Given that strong dependence of an FLD on both the strain state and the strain path, it is critical to realise the deformations under various proportional strain paths in the in-plane biaxial tensile test. In this study, three different stretching modes in a previously developed planar biaxial tensile rig, called stretching model-I, stretching model-II and stretching model-III, were applied to deform one type of cruciform specimen for AA5754 under an expected strain state of the equi-biaxial tension, the plane-strain tension and the uniaxial tension, respectively. The digital image correlation (DIC) technique was adopted for strain field measurement. By analysing the ratio and the linearity of the strain paths in the different zones within the gauge area of the cruciform specimens, it was found that, by using the stretching mode-I, the equi-biaxial strain state was obtained only in the central zone, and the corresponding strain path is linear. The plane-strain states were not achieved in any zones within the gauge area by using the stretching mode-II, and the corresponding strain paths are nonlinear. By using the stretching mode-III, the fracture occurred in a zone within the gauge area where the strain state is uniaxial and the corresponding strain path is linear, while the strain state in the central zone is close to the pure shear and the strain path is nonlinear.

© 2020 The Authors. Published by Elsevier B.V.
This is an open access article under the CC BY-NC-ND license (http://creativecommons.org/licenses/by-nc-nd/4.0/)
Peer-review under responsibility of the scientific committee of the 18th International Conference Metal Forming 2020

Keywords: Strain path; Strain state; In-plane biaxial tensile test; Cruciform specimen; Forming limit diagram

1. Introduction

Forming limit diagram (FLD) has been commonly used in evaluating the formability of metal sheets [1, 2], in which the limit strains at the onset of localised necking under various proportional strain paths are presented in the space of the major strain and the minor strain. Conventionally, an FLD is determined by either the Nakajima test [3] or the Marciniak test [4], and various strain states from uniaxial tension (β = -0.5) over plane strain tension (β = 0) to equi-biaxial tension (β = 1) are carried out by varying the geometry of the specimens [5], where β is the strain ratio of the strain path ($\beta = \Delta\varepsilon_2/\Delta\varepsilon_1$). However, inaccurate limit strains could be determined in the two tests due to the inevitable disadvantages, such as the bending of the sheets and the friction between the punch and the sheets in the Nakajima test, and the nonlinear strain paths in the two tests. In-plane biaxial tensile test is an alternative to determine an FLD, in which cruciform specimens are usually deformed under the plane stress condition. However, the in-plane biaxial tensile test has not been widely accepted due to the lack of a standard testing method.

Significant efforts have been dedicated for the development of the in-plane biaxial tensile tests for the formability evaluation [6]. The existing biaxial testing machines are mainly classified into three categories: (1) link-mechanism machines, (2) gear-mechanism machines and (3) stand-alone machines. One of the typical link-mechanism machines was proposed by Nagayasu et al. [7], to convert an uniaxial compression force into four output forces and to ensure equivalent displacement of two opposing grips. The ratio of strain path is controlled by adjusting the angle between the arm and the vertical axis and thus the load ratio between two axes of cruciform specimens.

2351-9789 © 2020 The Authors. Published by Elsevier B.V.
This is an open access article under the CC BY-NC-ND license (http://creativecommons.org/licenses/by-nc-nd/4.0/)
Peer-review under responsibility of the scientific committee of the 18th International Conference Metal Forming 2020
10.1016/j.promfg.2020.08.105

Similar machine was adopted by Seymen et al. [8] and Güle and Efe [9] for formability evaluation. There are also other link-mechanism machines which were proposed by Ferron and Makinde [10], Tasan et al. [11], Farhadzadeh et al. [12] and Barroso et al. [13]. However, only the strain paths with positive ratios in the righthand side of an LFD can be achieved in the link-mechanism machines, and the force transfer efficiency is quite low. Abu-Farha et al. [14] developed a gear-mechanism biaxial testing rig, in which the ratio of strain path can be controlled by adjusting gear ratios. With respect to the stand-alone machines, Zidane et al. [15] designed a servo-hydraulic testing device equipped with four independent dynamic actuators, and various strain paths were realised by controlling the displacement ratios imposed on two axes. Similar designs of the biaxial testing machines were also adopted by Xiao et al. [16], Schemmann et al. [17] and Kulawinski et al. [18].

In order to determine FLDs of metal sheets under various forming conditions, e.g. hot stamping, a novel planar biaxial tensile rig was proposed and patented by Shao et al. [19] to be used in the Gleeble. The in-plane biaxial tensile test system had been applied for the formability evaluation for aluminum alloy 6082 (AA6082) under the hot stamping conditions [20].

The aim of the study is to investigate the ratio and the linearity of the strain paths in the gauge area of the cruciform specimen in the in-plane biaxial tensile test. A new type of cruciform specimen for AA5754 was proposed and three different stretching modes in the patented planar biaxial tensile rig were applied to deform the cruciform specimens separately. Both the ratio and the linearity of the strain paths in different zones within the gauge area of the cruciform specimen were compared and analysed. This provides the basis for optimising the rig to generate a wider range of proportional strain paths.

2. Experimental method

2.1. Planar biaxial tensile rig and cruciform specimen design

A previously patented planar biaxial tensile rig [19, 20], which is capable of converting an uniaxial tensile force into planar biaxial tensile forces, was used for stretching cruciform specimens under the plane stress condition, as shown in Fig. 1(a). The arms of cruciform specimens were clamped with the runners which move along the parallel direction of the runner shafts. The top connectors between the runners and the top circle plate ensure to transform the rotational motion of the top circle plate into the linear motion of the runners. The top circle plate was connected to the bottom circle plate by the rectangle spline, and the bottom connector was used to transform the linear motion of the bottom runner along the tensile direction into the rotational motion of the bottom circle plate. The rig was assembled into the chamber of the Gleeble 3800 for the biaxial tensile tests.

Fig 1(b) shows the geometry and the dimensions of the cruciform specimens of AA5754 used in this study. The notch was designed at the corners of the arms to avoid the stress concentration at the locations. The thickness in a circular central area was decreased to localise the deformations, called the gauge area. The slits were added along the arms to reduce the constraints imposed on the deformations of the gauge area by the lateral stiffness of the arms, and thus to improve the uniformity of the strain distributions in the gauge area.

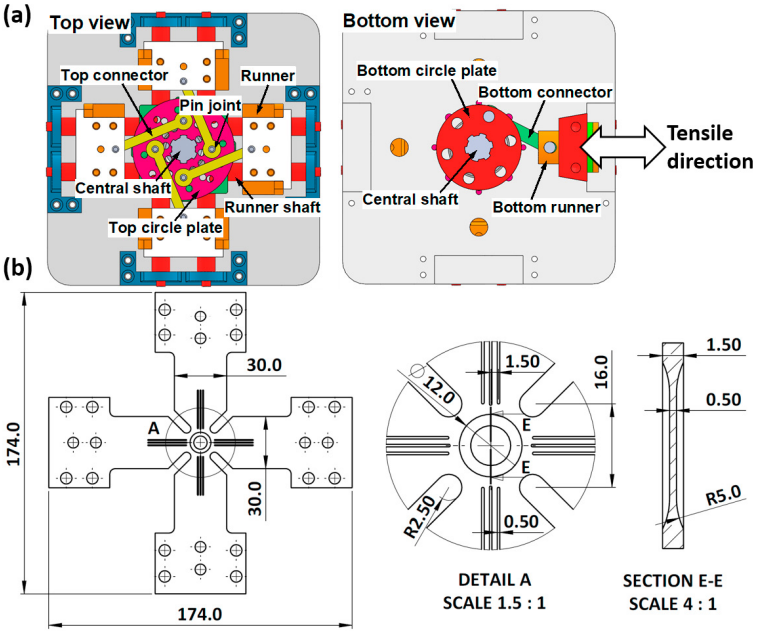


Fig. 1. (a1)-(a2) Top and bottom view of the previously patented planar biaxial tensile rig [19, 20] and (b) geometry and dimensions of the cruciform specimen.

2.2. Deformations under various loading states

All cruciform specimens were deformed at a constant speed of 15 mm/min in two axes of the specimens by using the stroke control method in the Gleeble. In order to generate the different loading states, three different stretching modes were utilised in the in-plane biaxial tensile tests, called stretching mode-I, stretching mode-II and stretching mode-III, as illustrated in Fig. 2. The stretching mode-I in Fig. 2(a) was used to generate

the equi-biaxial loading state, in which the four top connectors have the same length, and the pin joints on the central circular plate are symmetrical about the central shaft. The stretching mode-II in Fig. 2(b) was also used for the deformations under an expected loading state of the plane-strain tension by fixing the two runners along the vertical direction. Fig. 2(c) shows the stretching mode-III for the deformations under an expected loading state of the uniaxial tension, in which the two runners in the vertical direction can move freely along the parallel direction of the runner shafts. Among the three stretching modes, both the length of the top connectors and the locations of the pin joints on the top circle plate are the same.

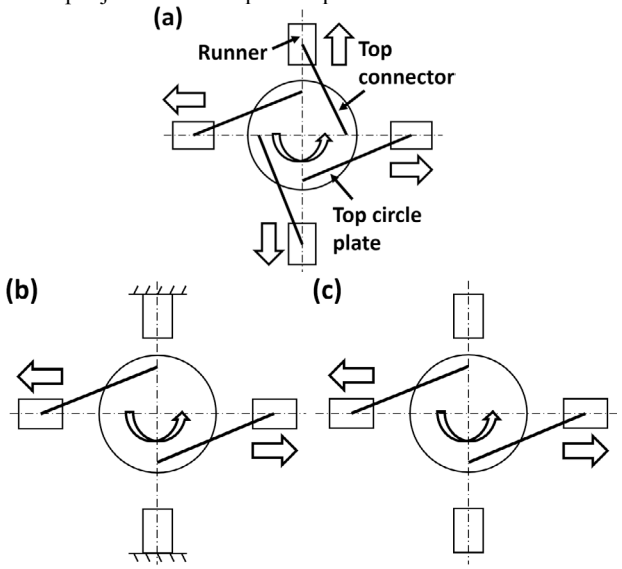


Fig. 2. Schematic diagrams illustrating (a) the stretching mode-I, (b) the stretching mode-II, and (c) the stretching mode-III to deform the cruciform specimens under an expected loading state of the equi-biaxial tension, the plane-strain tension and the uniaxial tension, respectively.

2.3. Strain field measurement

The digital image correlation (DIC) technique was applied for the measurement of deformation. After cleaning the surface of the specimens, the speckle patterns were prepared by spraying a black paint to generate randomly distributed black dots, against a thin layer of white background by spraying a white paint. A high-speed camera was used to capture the deformations and the images were taken at a constant frame rate of 125 frames per second (fps). Consequently, the images were processed in the commercial software ARAMIS by setting the facet size of 19 pixels and the facet step of 5 pixels.

3. Results and discussion

3.1. Deformations by the stretching mode-I

The cruciform specimens of AA5754 were deformed by using the stretching mode-I (Fig. 2(a)) in order to achieve the equi-biaxial tension in the gauge area. Fig. 3(a1)-(a4) shows the contours of engineering strain in thickness direction in the gauge area of a cruciform specimen, at the different normalised times (t/t_F), where t is the current time and t_F is the time at fracture. As expected, the deformations were mainly concentrated in the gauge area. In the strain contour at t/t_F = 100%, the crack initiation site was observed at the corner of the gauge area, where the thickness thinning is the maximum. Two circular zones with the same diameter of 2.5 × h (namely 1.25 mm), where h is the thickness of the specimen, were selected on specimen surface at the central site and the facture site before deformation, called the central zone and the fracture zone, respectively. The strain paths (hollow symbols) in the two zones were plotted in Fig. 3(b), in which the straight dashed lines were fitted by the experimental data before t/t_F = 30% with the least square method. It was observed that all experimental data in the central zone are on the fitted straight line with $1/n_C$ = 0.96, where n_C is the slope of the fitted straight line in the central zone. This means that the β of the strain path in the central zone is always 0.96, and thus the strain path is linear, and the corresponding strain state is equi-biaxial. In the fracture zone, however, a straight line with $1/n_F$ = 0.64 was fitted, where n_F is the slope of the fitted straight line in the fracture zone, and with the increase of deformation, an increasing diversion appeared between the experimental data and the fitted straight line. That is, the major strain within the fracture zone became much higher than the minor strain and thus, the β of the strain path in the fracture zone became much smaller than 0.64. This indicates that the strain path in the fracture zone is nonlinear, and the corresponding strain state is not equi-biaxial.

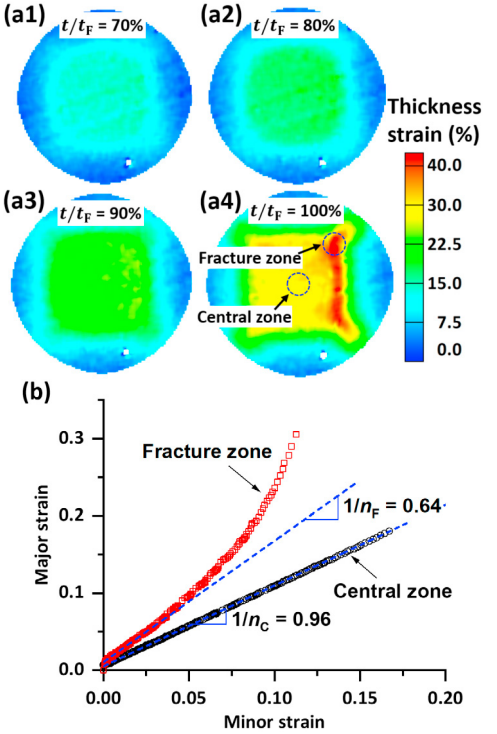


Fig. 3. (a1)-(a4) Contours of engineering strain in thickness direction in the gauge area of a cruciform specimen of AA5754 deformed by using the stretching model-I, and (b) strain paths in the central zone and the fracture zone separately.

3.2. Deformations by the stretching mode-II

The cruciform specimens of AA5754 were also deformed by using the stretching mode-II (Fig. 2(b)) in order to realise

the plane-strain tension in the gauge area. Fig. 4(a1)-(a4) shows the contours of engineering strain in thickness direction in the gauge area of a cruciform specimen at the different normalised times. Similar to the observations in the tests by using the stretching mode-I, the deformations were mainly concentrated in the gauge area. In the strain contour at t/t_F = 100%, a crack initiation site was observed, and two circular zones with the same diameter of 1.25 mm, namely the central zone and the fracture zone, were selected on specimen surface at the central site and the crack initiation site respectively. Fig. 4(b) plotted the strain paths (hollow symbols) in the two zones and the fitted straight lines (dashed blue lines) by the experimental data before t/t_F = 30% separately. With the increase of the deformations, all experimental data in both the central zone and the fracture zone deviated from the fitted straight lines gradually. This indicates that the strain path in either the central zone or the fracture zone is nonlinear. In addition, at the initial time of deformation ($t/t_F \leq 30\%$), the β of the strain path in the central zone and the fracture zone is about -0.50 and -0.26 respectively, and the β increased with the increase of deformation. This means that the corresponding strain state in either the central zone or in the fracture zone is not plane-strain state.

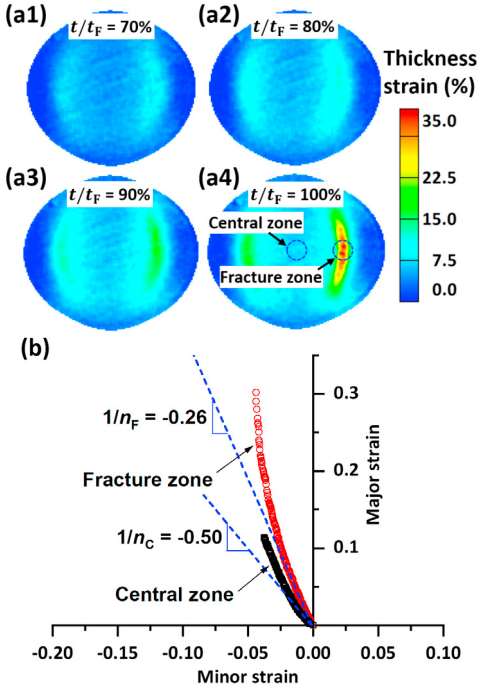


Fig. 4. (a1)-(a4) Contours of engineering strain in thickness direction in the gauge area of a cruciform specimen of AA5754 deformed by using the stretching mode-II, and (b) strain paths in the central zone and the fracture zone separately.

3.3. Deformations by the stretching mode-III

The stretching mode-III (Fig. 2(c)) was also applied to deform the cruciform specimens of AA5754 in order to carry out the uniaxial tension in the gauge area. Fig. 5(a1)-(a4) shows the contours of engineering strain in thickness direction in the gauge area of a cruciform specimen at the different normalised times, in which the crack initiation site was observed in the strain contour at t/t_F = 100%. A central zone and a fracture zone with the same dimeter of 1.25 mm were selected at the central site and the fracture site, respectively. The strain paths (hollow symbols) in the two zones were plotted in Fig. 5(b), with the fitted straight lines (dashed blue lines) by using the experimental data before t/t_F = 30% separately. It was observed that the β of the strain path in the fracture zone is about -0.51 before t/t_F = 90%, which indicates that the strain path in the fracture zone is linear, and the corresponding strain state is uniaxial before appearance of instability. For the strain path in the central zone, however, the β is about -0.68 before t/t_F = 90%, and with the crease of time, the experimental data deviated from the fitted line and thus the β decreased gradually. This means that the strain path in the central zone is nonlinear, and the corresponding strain state is not uniaxial, but close to the pure shear (β = -1).

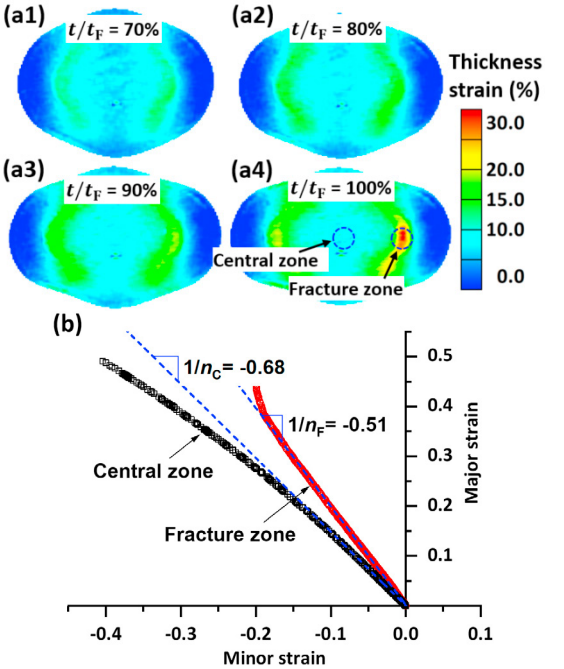


Fig. 5. (a1)-(a4) Contours of engineering strain in thickness direction in the gauge area of a cruciform specimen of AA5754 deformed by using the stretching mode-III, and (b) strain paths in the central zone and the fracture zone separately.

3.4. Discussion

By using the stretching model-I, only the strain state in the central zone of the cruciform specimen is equi-biaxial, as shown in Fig. 3(b). This means that the shear stress in the central zone within the gauge area of the cruciform specimen is very low, and thus the major stress is almost equal to the minor stress. The same observation can also be found in [21]. Therefore, one of the preconditions of determining the limit strains under the proportional equi-biaxial strain path is that the fracture initiation site must appear in the central zone of the cruciform specimen.

Neither the strain state is the plane-strain state nor the strain path is proportional in the gauge area of the specimens when using the stretching mode-II. In fact, the corresponding minor strains within the gauge area are negative, as shown in Fig.

4(b). This is likely because the materials in the gauge area are stretched and deformed as well along the direction from the fixed runners to the centre of the specimens. In order to realise the deformations under the plane-strain state, the two runners in the vertical direction may not be fixed, but be stretched with proportional displacements as well.

By using the stretching mode-III, the uniaxial strain state was observed in the fracture zone rather than in the central zone where the strain state approaches the pure shear, as shown in Fig. 5(b). This indicates that the two arms of the specimens in the vertical direction of the freely moved runners affect the deformations in the gauge area, and the zones at a distance from the centre of the specimens can be deformed under the uniaxial tension.

4. Conclusions

In order to perform the deformations under various proportional strain paths for evaluating the formability of metal sheets, the cruciform specimens of AA5754 were deformed by using the three different stretching modes in the previously patented planar biaxial tensile rig, namely the stretching mode-I, the stretching mode-II and the stretching mode-III. After analysing the ratio and the linearity of the strain paths in the different zones within the gauge area of the cruciform specimens, the following conclusions can be drawn:

1) By using the stretching mode-I, the equi-biaxial strain state was obtained only in the central zone within the gauge area, and the corresponding strain path is linear. However, in the other zones within the gauge area, neither the strain state is equi-biaxial nor the strain path is linear due to the presence of the shear stress;
2) By using the stretching mode-II, the linear plane-strain path was not obtained in any zones within the gauge area. In fact, the minor strains are negative and the corresponding strain paths are nonlinear;
3) By using the stretching mode-III, the fracture occurred in a zone within the gauge area, where the strain state is uniaxial and the corresponding strain path is linear. However, the strain state in the central zone is close to the pure shear, and the corresponding strain path is nonlinear.

Acknowledgements

Financial support from EPSRC under the grant number EP/R001715/1 on “Lightform: Embedding Materials Engineering in Manufacturing with Light Alloys” is gratefully acknowledged. R. Zhang appreciates financial support from the CSC-Imperial Scholarship (Grant no. 201700260069).

References

[1] Keeler SP. Determination of forming limits in automotive stampings. Sheet Metal Industry 1965;42:683-91. doi:10.4271/650535
[2] Goodwin GM. Application of strain analysis to sheet metal forming problems in the press shop. SAE Technical Paper 1968:380-7. doi:10.4271/680093
[3] Nakazima K, Kikuma T, Hasuka K. Study on the formability of steel sheets. Yamata Technical Report 1968:8517-30.
[4] Marciniak Z, Kuczyński K, Pokora T. Influence of the plastic properties of a material on the forming limit diagram for sheet metal in tension. Int J Mech Sci 1973;15:789-800.
[5] BS EN ISO 12004, Metallic materials — Sheet and strip — Determination of forming-limit curves Part 2: Determination of forminglimit curves in the laboratory, 2008. doi:10.3403/bseniso12004.
[6] BS ISO 16842, Metallic materials — Sheet and strip — Biaxial tensile testing method using a cruciform test piece, 2014. doi:10.3403/30246886.
[7] Nagayasu T, Takahashi S, Kuwabara T. Development of compact biaxial tensile testing apparatus using conventional compression testing machine and evaluation of the test results. International Deep-Drawing Group (IDDRG); 2010.
[8] Seymen Y, Güler B, Efe M. Large Strain and Small-Scale Biaxial Testing of Sheet Metals. Experimental Mechanics 2016;56:1519-30. doi:10.1007/s11340-016-0185-7.
[9] Güler B, Efe M. Forming and fracture limits of sheet metals deforming without a local neck. J Mater Process Tech 2018;252:477-84. doi:10.1016/j.jmatprotec.2017.10.004.
[10] Ferron G, Makinde A. Design and development of a biaxial strength testing device. Journal of Testing and Evaluation 1988;16:253-6. doi:10.1520/jte10375j.
[11] Tasan CC, Hoefnagels JPM, Quaak G, Geers MGD. In-plane biaxial loading of sheet metal until fracture International Congress and Exposition on Experimental and Applied Mechanics, Orlando, Florida; 2008. p. 2-5.
[12] Farhadzadeh F, Salmani-Tehrani M, Tajdari M. Determining biaxial tensile stresses by fracture cruciform specimen at different temperatures and strain rates for Ti–6Al–4V alloy. Journal of the Brazilian Society of Mechanical Sciences and Engineering 2018;40:532. doi:10.1007/s40430-018-1455-3.
[13] Barroso A, Correa E, Freire J, París F. A device for biaxial testing in uniaxial machines. Design, manufacturing and experimental results using cruciform specimens of composite materials. Experimental Mechanics 2018;58:49-53. doi:10.1007/s11340-017-0327-6.
[14] Abu-Farha F, Hector L, Khraisheh M. Cruciform-shaped specimens for elevated temperature biaxial testing of lightweight materials. JOM – Aluminium: Shaping and Forming 2009;61:48-56. doi:10.1007/s11837-009-0121-8.
[15] Zidane I, Guines D, Leotoing L, Ragneau E. Development of an in-plane biaxial test for forming limit curve (FLC) characterization of metallic sheets. Measurement Science and Technology 2010:055701. doi:10.1088/0957-0233/21/5/055701.
[16] Xiao R, Li X-X, Lang L-H, Chen Y-K, Yang Y-F. Biaxial tensile testing of cruciform slim superalloy at elevated temperatures. Materials & Design 2016;94:286-94. doi:10.1016/j.matdes.2016.01.045.
[17] Schemmann M, Lang J, Helfrich A, Seelig T, Böhlke T. Cruciform Specimen Design for Biaxial Tensile Testing of SMC. J Compos Sci 2018;2:12.
[18] Kulawinski D, Ackermann S, Seupel A, Lippmann T, Henkel S, Kuna M, Weidner A, Biermann H. Deformation and strain hardening behavior of powder metallurgical TRIP steel under quasi-static biaxial-planar loading. Mater Sci Eng A 2015;642:317-29. doi:10.1016/j.msea.2015.06.083.
[19] Lin J, Li N, Shao Z, Qian B. Planar test system. United States 'Patent' US 20180238784 A1, Aug. 23; 2018.
[20] Shao Z, Li N, Lin J, Dean T. Development of a new biaxial testing system for generating forming limit diagrams for sheet metals under hot stamping conditions. Experimental Mechanics 2016;56:1489-1500. doi:10.1007/s11340-016-0183-9.
[21] Zhang S, Leotoing L, Guines D, Thuillier S, Zang S-L. Calibration of anisotropic yield criterion with conventional tests or biaxial test. Int J Mech Sci 2014;85:142-51. doi:10.1016/j.ijmecsci.2014.05.020.